A Study on the Effect of Potentiostatically Grown Gold Oxide Films on the Oxidation of Phenol in Base

P I Iotov and S V Kalcheva

University of Chemical Technology and Metallurgy, Sofia, Bulgaria
E-mail: pi@uctm.edu

Received: 6 September 2000

The general behaviour of potentiostatically grown gold oxide films during the oxidation of phenol in basic solutions has been studied using cyclic voltammetry. No catalytic activity is observed and phenol oxidation is prevented when the oxide film consists of both α- and β-oxides. The depletion of β-oxide is accompanied by rapid electrode passivation, showing that the presence of $Au(OH)_3$ is essential for the oxidation process to take place. A tentative reaction mechanism based on the IHOAM model of electrocatalysis is proposed to account for the participation of the redox mediator couple Au(I)/Au(III).

In solutions having high concentrations of $KClO_4$ or KCl and short reaction times chlorination occurs at gold oxide electrode films, without polymerization at temperatures lower than 308 K and 321 K respectively. Oxidation and chlorination reactions occur with apparent activation energies of *ca* 17 and 70 kJ mol^{-1} respectively : this indicates that oxidation is favoured at lower concentrations of the additives.

Aqueous wastes containing phenolic contaminants are resistant toward purification and toxic toward microorganisms in conventional biological treatment reactions. As a 'front-end' technology aimed at their detoxification rather than complete mineralization, electrolysis can be used ahead of biological treatment (1). In general, phenols cause deactivation of the anode, reportedly via formation of polyoxyphenylene (POP) deposited when phenoxy radicals attack unreacted substrate. Deactivation by the polymer occurs more slowly at oxide-based electrodes (2, 3) and their activity varies greatly with the nature of the oxide (4). Although gold is the noblest and most inert of metals, and is a very weak chemisorber, it displays a very wide range of electrocatalytic activity especially in base (5). Electrocatalytic processes have been widely studied, firstly to understand their reaction mechanism better and secondly to improve their relevance to industrial applications. The reaction mechanisms can be studied by modifying the structure of the electrode surface in order to influence the adsorption of the different species involved in the electrocatalytic processes. One way of modifying the catalytic surface is the oxidation of the metal by potentiostatic or potentiodynamic polarization. Potentiostatic pretreatment of a polycrystalline gold (pc-Au) electrode at high overpotentials results in thick film growth consisting of α– and β-oxides (6, 7). The objective of this study was to increase our knowledge of the mechanism of phenol oxidation at potentiostatically grown gold oxide films in alkaline solutions of various compositions and especially to examine the effect of additives on the thickness and catalytic properties of the oxide.

EXPERIMENTAL

Cyclic voltammetry was used to study the redox behaviour of either the electrode surface or solution species. Experiments were carried out with three glass cells and conventional electrochemical equipment. The electrode set consisted of a working electrode made of gold-plate with a geometric area of 1 cm^2, a gold counter electrode and an Hg/HgO/1M KOH reference electrode. All potentials are reported against the reversible hydrogen electrode (RHE). To achieve

sustainability of the working electrode area and the roughness factor, 1000 cycles were applied between 0 and 1.75 V with a scan rate (s) of 5.00 V s^{-1} in the first cell containing 1 M KOH. This preliminary treatment (8) lead to a constant roughness factor, its value depending on the composition of the background electrolyte used in the subsequent experiments. It was close to 1.6 in 0.05 M KOH, close to 1.8 in 0.05 M KOH + 0.05 M $KClO_4$ and *ca* 2.0 in 0.05 M KOH + 0.05 M KCl. Prior to anodization the real surface area of pc-Au was determined in the first cell at 298.2 K in a nitrogen atmosphere, a charge of 0.386 mC cm^{-2} being necessary to form a monolayer of oxygen in the form of $Au(OH)_2$ and allowing for the double layer charging (reference 8 and references therein). The working electrode was immersed in the second cell, which had been purged with nitrogen. To grow β-oxide, the gold electrode surface was subjected to preliminary potentiostatic anodization at 2.50 V. The effect of preanodization time (t_{ox}) and temperature (T) on the growth of β-oxide film and on phenol oxidation was investigated in the ranges from 10 to 738 s (9) and 288.2 – 338.2 K. During polarization the inflow of gas was interrupted. To avoid the effect of molecular oxygen on the oxide reduction charge density (q_{ox}), the negative sweep was arrested at *ca* 1.75 V for 1800 s with resumed nitrogen bubbling. The same procedure was applied prior to the transfer of the working electrode to the third cell where the influence of β-oxides on the oxidation of phenol was studied. Based on the results of preliminary experiments, t_{ox} = 738 s was selected, and 0.01 M aqueous phenolic solutions were used in the corresponding background electrolyte, purged with nitrogen prior to the experiments. Cyclic voltammetry was applied starting at 1.75 V in a positive direction to reach the upper potential limit of 2.50 V. The lower limit was determined in the course of studying the reduction of the oxides. It was found that when the potential was cycled down to 1.05 V, α-oxide was reduced while β-oxide remained on the electrode surface. The scan rate was varied from 0.05 to 0.50 V s^{-1}. Experiments were performed in triplicate to ensure reproducibility. The solutions investigated were prepared from doubly distilled water, 'Chemapol' analytical grade phenol (PhOH), 'Merck' p.a. KOH, and VEB 'Chemie– Apolda' suprapur grade $KClO_4$ and KCl.

RESULTS AND DISCUSSION

The general behaviour of the pc-Au oxide electrodes in the phenol oxidation process is determined by the

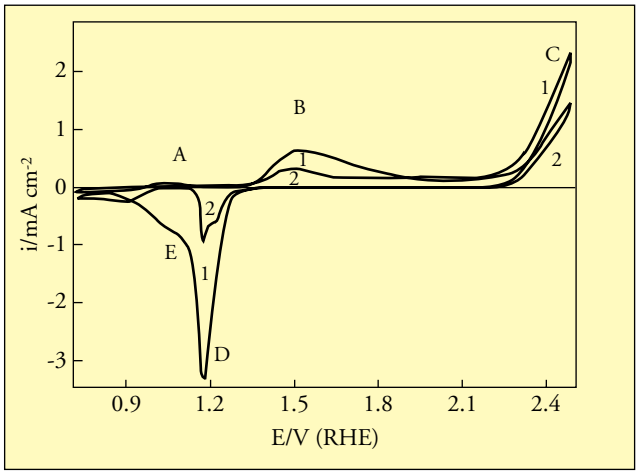

Figure 1 *Typical cyclic voltammograms of preanodized pc-Au in 0.05 M KOH + 0.01 M phenol recorded at 0.05 V s^{-1} in the potential range from 0.70 to 2.50 V vs RHE, T = 308.2 K: (1) first scan; (2) second scan*

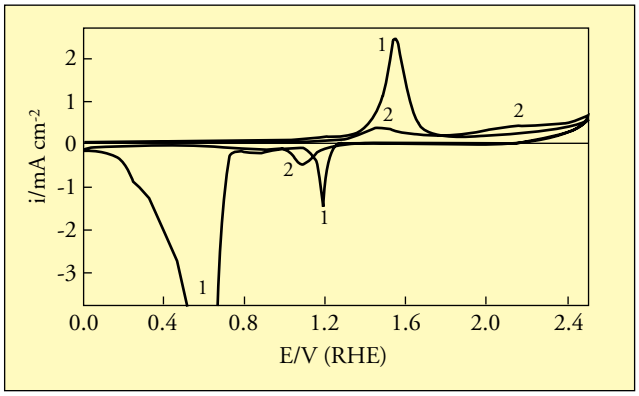

Figure 2 *Cyclic voltammograms of preanodized pc-Au in 0.05 M KOH + 0.01 M phenol at 0.05 V s^{-1}, in the potential range from 0 to 2.50 V vs RHE, T = 308.2 K: (1) first scan; (2) second scan*

potential range limits investigated. The impact of the lower potential limit (E_l) variation at constant upper potential limit (E_u) is illustrated in Figures 1-4. Two subsequent cyclic voltammograms (CV's) of gold oxide electrode in alkaline phenolic solution, in the potential range 0.70 – 2.50 V are presented in Figure 1. The plateau A is due to the slow oxidation of phenol, peak B is a superimposition of the fast phenol oxidation on α-oxide growth, peak C shows oxygen evolution (OE), and peak D is reduction of α-oxide while wave E presents the reduction of β-oxide. As seen from Figure 1, anodic and cathodic currents are lower in the second scan than in the first. This is a direct consequence of surface fouling preceded by complete reduction of α-oxide and partial reduction of β-oxide. If E_l of the

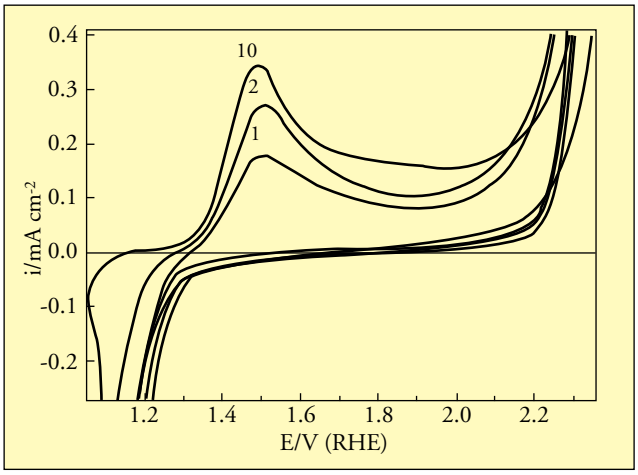

Figure 3 *Current – potential response of preanodized pc-Au to successive potential scanning at 0.10 V s^{-1} in the range from 1.05 to 2.50 V vs RHE, in 0.05 M KOH + 0.01 M phenol, T = 298.8 K: (1) first scan; (2) second scan; (10) tenth scan*

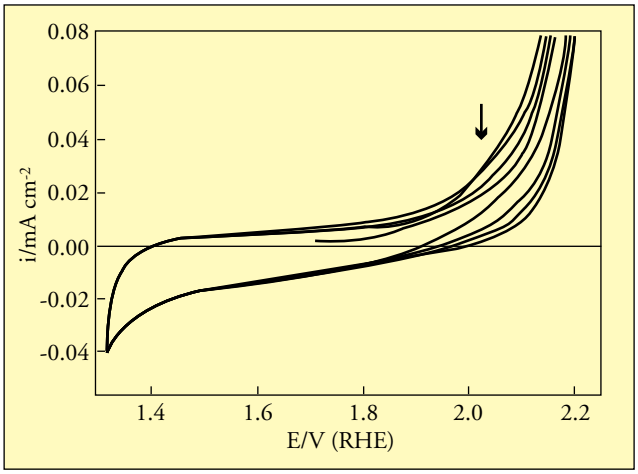

Figure 4 *Cyclic voltammograms of preanodized pc-Au in 0.05 M KOH + 0.01M phenol, at 0.10 V s^{-1} in the potential range from 1.30 V to 2.50 V vs RHE, T = 298.8 K*

applied potential permits the total reduction of surface oxides, the catalytic surface is rapidly deactivated due to polymer blocking of the *active* sites – see Figure 2. This passivation is eliminated when the lower potential limit is fixed at 1.05 V, *ie* the reduction of β-oxide is prevented (6). The general current-potential response of gold oxide electrode to ten successive potential scans is illustrated in Figure 3. The peak current density (i_p) increases on successive scanning and a reproducible current-potential curve is reached. A well-defined oxidation peak is observed at *ca* 1.5 V, *ie* in the area corresponding to peak B in Figure 1. If E_l is further increased to 1.30 V, maintaining E_u at 2.50 V, then no catalytic activity is observed, as shown in Figure 4; the arrow indicates a current density decrease accompanied by a potential shift of OE. This figure suggests that the co-existence of both α- and β-oxides prevents the phenol oxidation process occurring.

When E_u = 1.57 V, which is below that of oxygen evolution, and E_l is 1.05 V, higher current densities are recorded at the gold oxide anode. The initial i_p in Figure 5a is significantly higher than that recorded under the conditions represented by Figure 3. On subsequent scanning i_p gradually decreases (scans 2 and 3). In Figure 5a scan 4 reveals the residual quantities of α- and β-oxides on the same electrode as measured after its immersion in 0.05 M KOH. Comparison of the reduction profiles of scans 1-4

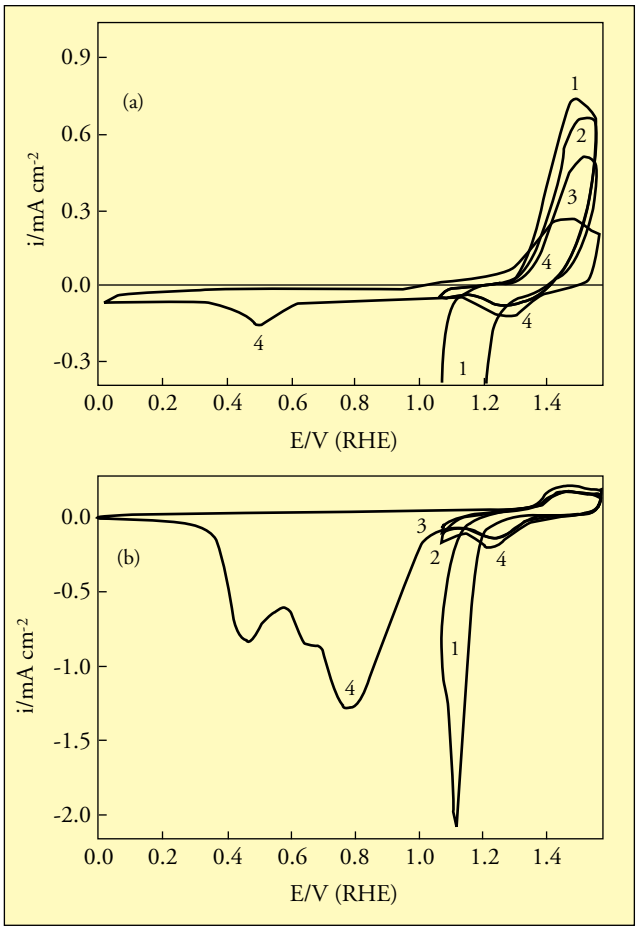

Figure 5 *Cyclic voltammograms of preanodized pc-Au in 0.05 M KOH at 0.05 V s^{-1}, in the potential range from 1.05 V to 1.57 V vs RHE, T = 308.2 K: (a) three subsequent scans with 0.01 M PhOH followed by a scan in the range from 1.57 V to 0 V in absence of PhOH; (b) four analogous scans recorded in 0.05 M KOH*

(Figure 5a) demonstrates that in the fourth scan the quantity of α-oxide is higher than during the preceding scans. In addition, the juxtaposition of scans 4 in Figures 5a and 5b reveals that in the presence of phenol β-oxide is depleted. The results obtained in presence of $KClO_4$ and KCl additives are of a similar type to those described above.

Figures 6a and 6b show CV's recorded in the presence of added $KClO_4$ and KCl respectively. The experimental conditions are identical with those used to obtain the results illustrated in Figure 3, and this permits a direct comparison of the i/E-responses. The CV's have a similar form and i_p is observed at *ca* 1.50 V. The values of i_p are the highest in KOH and the lowest in KOH + KCl. This is valid for all experiments carried out in the temperature range 288.2 – 308.2 K. At higher temperatures the peak current densities in

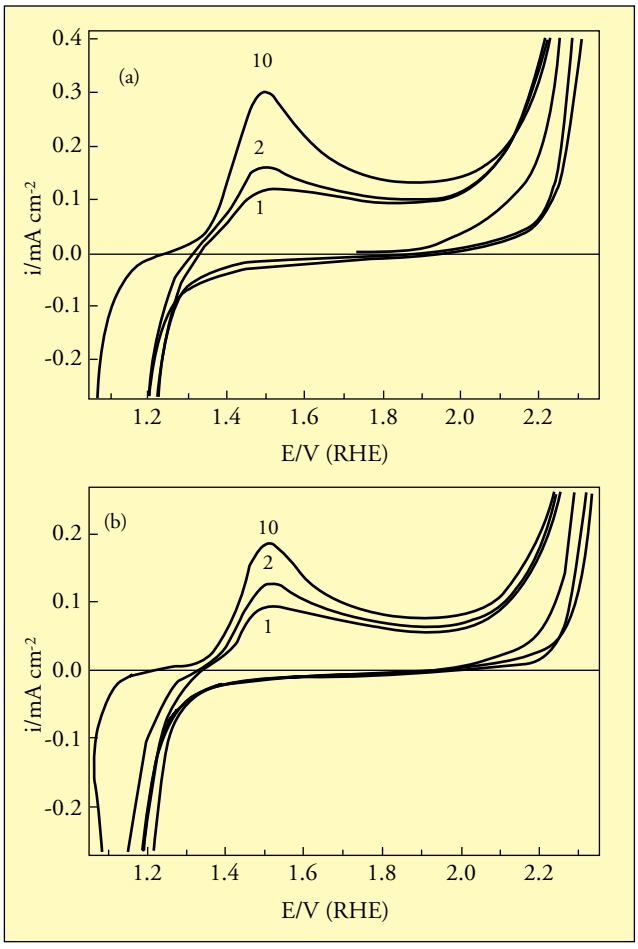

Figure 6 *Current-potential response of preanodized pc-Au-electrode to successive (1-10) scans at 0.10 V s^{-1} in the range from 1.05 V to 2.50 V vs RHE: (a) T=298.8 K, 0.05 M KOH + 0.05 M $KClO_4$; (b)T = 299.9 K, 0.05 M KOH + 0.05 M KCl*

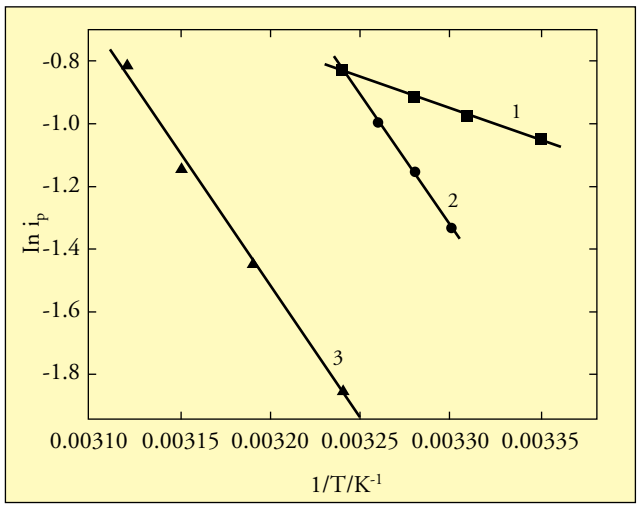

Figure 7 *Plots of ln i_p vs 1/T for the oxidation of 0.01 M phenol at preanodized pc-Au-electrode in the potential range from 1.05 V to 2.50 V vs RHE: (1) 0.5 M KOH; (2) 0.05 M KOH + 0.05 M $KClO_4$; (3) 0.05 M KOH + 0.05 M KCl*

KOH and KOH + $KClO_4$ decrease on successive scanning and no reproducible CV's are recorded. Similar behaviour is observed for KOH + KCl but at temperatures higher than 321.2 K. Polymer fouling was attributed to the effect of temperature on the partial pressure of dissolved oxygen.

The impact of temperature variation on phenol oxidation on potentiostatically grown oxide film was verified by recording CV's at temperatures (T) between 298.2 and 338.2 K in the potential range 1.05 V – 2.50 V. The data obtained are presented as Arrhenius plots in Figure 7. The apparent activation energies ($E^{\neq}$), calculated on the basis of the reproducible curves are 16.6 kJ mol^{-1} (KOH), 69.4 kJ mol^{-1} (KOH+ $KClO_4$) and 70.6 kJ mol^{-1} (KOH + KCl). On further increase in temperature electrode fouling is observed. At lower temperatures in KOH and KOH + $KClO_4$, i_p decreases with temperature increase, while in KOH + KCl it does not change. This suggests the occurrence of a multistep process. Additional experimental evidence is provided by the effect of scan rate (s) variation on i_p and the peak potential (E_p). In KOH, CV's at a preoxidized gold electrode showed an oxidation peak that increased in amplitude and moved to more positive potentials with increased sweep rate, typical of a totally irreversible system (10). The linear dependence of i_p on $s^{1/2}$, as predicted by the Randles-Sevcik equation (11), shows that the oxidation is diffusion controlled at a phenol concentration of 0.01 M l^{-1}. This is consistent with Gattrell's (2) observation

that phenol undergoes diffusion-controlled oxidation to benzoquinone (BQ). At higher potentials, as the reaction proceeds in the oxygen-evolution region, it may be presumed that peroxide intermediates and/or hydroxyl radicals are involved as indirect oxidants. Their generation occurs through diffusion controlled oxygen reduction. The study of the scan rate effect on the oxidation process in presence of additives demonstrates that the reaction path in the presence of $KOH/KClO_4$ involves a reversible charge transfer followed by an irreversible chemical reaction. The voltammetric behaviour in KOH/KCl depends both on charge transfer- and chemical kinetics. These conclusions and the very close $E^{\neq}$-values determined in presence of added $KClO_4$ or KCl (Figure 7) lead to the assumption that different processes take place as compared to those in KOH.

The general concepts of the mechanism of phenol oxidation in the media studied require additional information on the kinetics of oxide growth. Some of the results on the kinetics of potentiostatic oxide growth at gold in KOH, $KOH/KClO_4$, and KOH/KCl at a polarization potential of 2.50 V and 308.2 K are illustrated in Figure 8. The plots $1/q_{ox}$ *vs* log t_{ox} indicate that the formation of gold oxide films is inversely logarithmic with time (4) and the process is limited by the rate of escape of the cation from the metal into the oxide. It is seen that two distinguishable linear regions with different slopes are indicated with

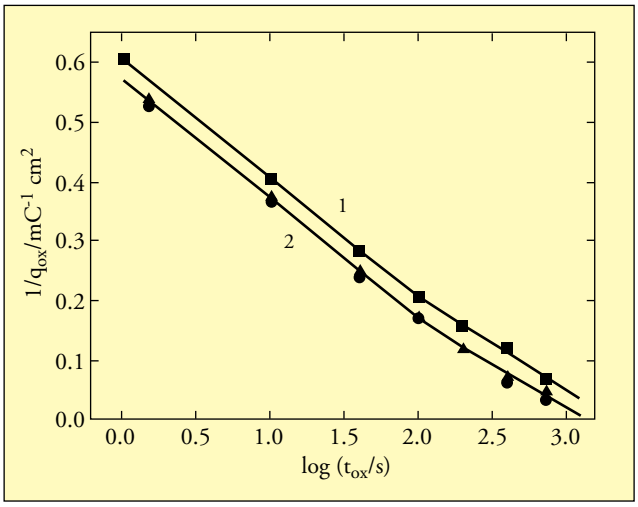

Figure 8 *Oxide growth at pc-Au in 0.05 M KOH (1, ■), 0.05 M KOH + 0.05 M $KClO_4$ (2, ●), and 0.05 M KOH + 0.05 M KCl (2, ▲) at 308.2 K and polarization potential of 2.50 V expressed as 1/ q_{ox} vs log t_{ox}. The inflection point between the linear regions of (1) and (2) is found close to $1/q_{ox}$ = 0.2 mC^{-1} cm^2.*

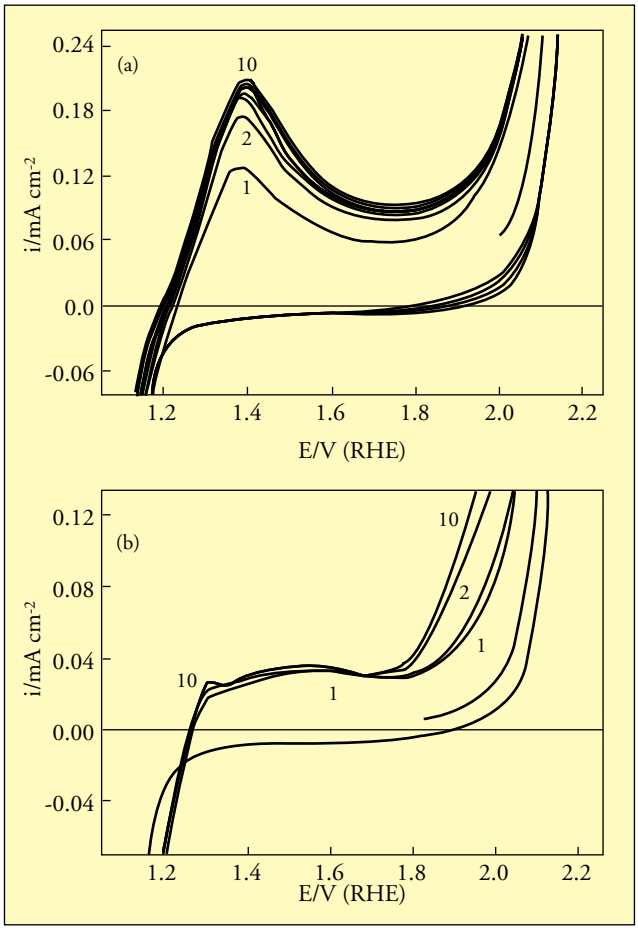

Figure 9 *Current-potential response of preanodized pc-Au-electrode to successive (1-10) scans at 0.05 Vs^{-1} in the range from 1.05 V to 2.50 V vs RHE, T = 307.9 K; (a) 0.05 M KOH + 0.01M PhOH; (b) 0.05 M KOH*

an inflection point found close to $1/q_{ox}$ = 0.2 mC^{-1} cm^2. The plots indicating oxide growth in $KOH/KClO_4$ and KOH/KCl actually coincide as shown by curve 2. The latter lies close to that obtained in KOH. In addition, the slopes of the linear regions in all media investigated are identical. The first lines correspond to the growth of α- and initial β-oxide films, while the second linear regions demonstrate the further development of β-oxides. Figure 8 shows that in presence of added $KClO_4$ or KCl the β-oxide is of identical composition but of different thickness to that obtained in KOH alone. This conclusion is supported by reference data on the thermodynamic properties of Au-Cl-H_2O system (12). Due to the powerful solubilizing effect of Cl^- ions, gold may dissolve at *ca* pH 12 with a +3 oxidation state and subsequent tetrachloroaurate(III) ion

($AuCl_4^-$) formation. In accord with the diagram E-pH for this system at E > 0.95 V and at 8 < pH < 13, $AuCl_4^-$ is transformed into $Au(OH)_3$. The total thickness of the oxide layer grown at 308.2 K and t_{ox} = 738 s was calculated (13) to be *ca* 13.5 Å (KOH), 55.7 Å (KOH/$KClO_4$) and 65.9 Å (KOH/KCl).

An oxide film present on the pc-Au surface influences the mechanism of redox reactions (14) by:

- affecting the energetics of the reaction at the double layer,
- changing the electronic properties of the metal surface,
- imposing a barrier to charge transfer across the surface oxide film,
- influencing the adsorption behaviour of reaction intermediates at the catalytic surface.

The anodization causes a change in the conducting properties of the electrode as the mixed oxide film eliminates the occurrence of charge transfer from the bulk of the metal to the electrode surface. The presence of the oxide film imposes a barrier to the charge transfer as indicated by the absence of any anodic peak in Figure 4.

The scan rate effect on the catalytic properties of the oxide film is illustrated in Figures 9 and 10. The potential is varied with a rate from 0.005 to 0.20 Vs^{-1}. Figure 9a shows that at 0.05 Vs^{-1} the anodic current grows continuously, but the reproducible value reached remains lower compared to that at 0.10 Vs^{-1} (Figure 3). This is also valid for the current-potential response in the absence of phenol as seen from Figure 9b. The comparison of the currents in Figures 3, 4 and 9(a, b) indicates that the anodic currents recorded in the presence of phenol are determined by its oxidation. The currents in Figure 10a are even greater. The scan rate used in this case is favourable for the formation of phenoxy radicals but too high for oxygen reduction, resulting in initial fouling of the electrode surface. This leads to the appearance of the new maximum at *ca* 1.95 V. The interpretation just presented is further verified by the experiments illustrated in Figure 10b. In this case, the negative profile (between points a and b) is recorded with a scan rate of 0.005 Vs^{-1} to provide extra HO_2^-, while the subsequent positive scanning proceeds with 0.05 Vs^{-1}. Thus, the peak current density reached is as high as that of the reproducible curve in Figure 9a. Curve 2 in Figure 10b shows that the current recorded is lower when the scan rate is preserved unchanged.

In this context, the experimental results described above permit the elucidation of some mechanistic aspects of the processes occurring at preanodized pc-Au electrodes. In basic media the anodic oxidation of

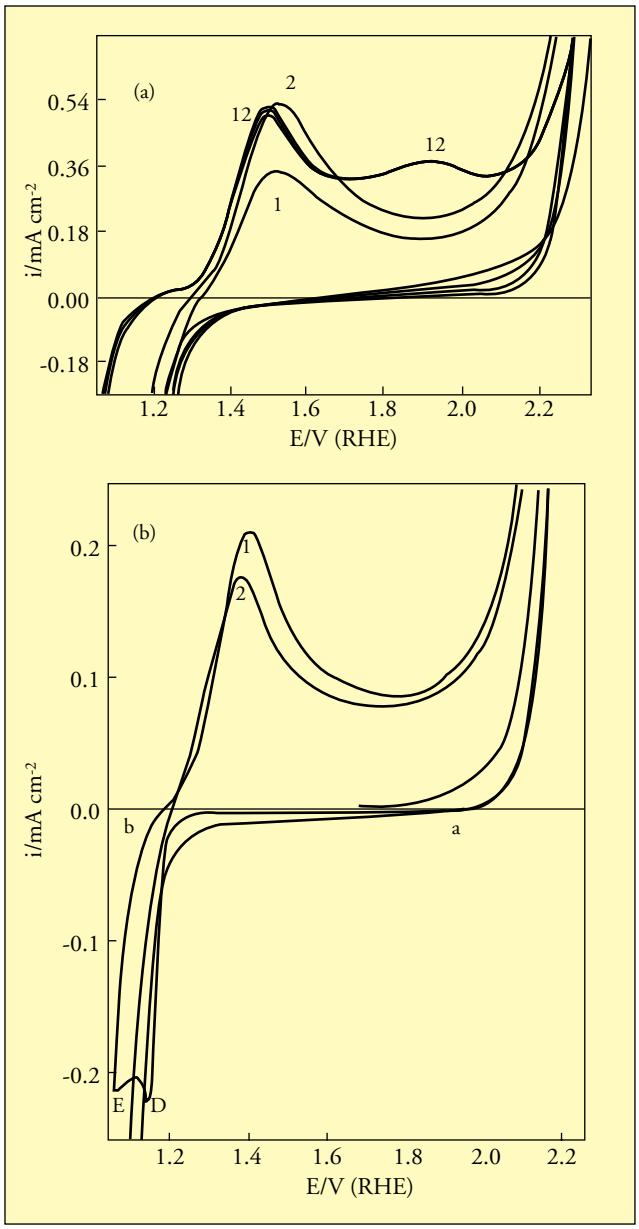

Figure 10 *Current-potential response of preanodized pc-Au-electrode to successive scans in 0.05 M KOH + 0.01M PhOH in the potential range from 1.05 V to 2.50 V vs RHE: (a) twelve successive scans at 0.20 Vs^{-1}, T = 308.7 K; (b) two successive scans at 0.05 Vs^{-1}, T= 307.9 K; the first cathodic profile recorded with a rate of 0.005 Vs^{-1} between points a and b*

phenol at an oxide-free electrode surface is preceded by the formation of phenoxide ions (15). A rapid POP polymerization process (16) follows their adsorption. On a preanodized pc-Au electrode an uninhibited oxidation occurs and reproducible curves are recorded in the potential range from 1.05 to 2.50 V. This

indicates that phenol oxidation proceeds selectively only at high overpotentials under conditions of oxygen evolution. Evolved oxygen undergoes cathodic reduction resulting in the formation of various products. In alkaline solutions oxygen reduction (OR) proceeds with hydrogen peroxide ion (HO_2^-) formation as an intermediate or end product. The clean electrode surface favours HO_2^- decomposition to HO^- and $O^\bullet$, while in presence of oxides or impurities, the peroxide path predominates (17). The overlayer provides for oxygen diffusion and its subsequent reduction is expected to occur at the α-oxide-free electrode surface at *ca* 1V (18). Furthermore, the surface overlayer is hydrous oxide, probably having the composition $Au_2(OH)_9^{3-}$ or $Au(OH)_3$, which stereochemically hinders adsorption of the phenol and eliminates polymerization fouling. The overlayer is known to have a porous structure, *ie* it acts as a membrane permeable for smaller ions and molecules and is impermeable to phenol. It is also well known that $Au(OH)_3$ has the properties of a weak acid which coordinates HO^- or phenoxide ions: this is supported by the fact that Au(III) is prone to coordinate ligands which contain oxygen (19). Electrocatalytic phenomena at noble metal electrodes may be interpreted on the basis of the incipient hydrous oxide/adatom mediator (IHOAM) model. This model of electrocatalysis has been elaborated by Burke *et al* over the last 15 years (5, 6, 20–23) and was originally proposed to explain the poor chemisorbing properties of gold. In this approach the metal atoms at the surface are regarded as having a degree of mobility and a range of chemical reactivities. To account for the experimental results described above, two schemes may be proposed. The overall processes for KOH solution in the potential range from 1.05 to 2.50 V are assumed to proceed in accordance with the following sequence:

1 Phenoxide ion formation and complexation at the overlayer:

$$PhOH + HO^- \rightarrow PhO^- + H_2O \quad (1)$$

$$Au(OH)_4^- + PhO^- \rightarrow Au(OH)_3...(PhO^-) + HO^- \quad (2)$$

where, $Au(OH)_3...PhO^-$ designates a complex in the vicinity of the electrode surface.

2 Oxygen adsorption and reduction processes:

$$Au(OH)_3...(PhO^-) + O_2 \rightarrow {}_{ads}(O_2)Au(OH)_3...(\ PhO^-) \quad (3)$$

$${}_{ads}(O_2)Au(OH)_3...(PhO^-) + e^- \rightarrow {}_{ads}(O_2^-)Au(OH)_3 ...(\ PhO^-) \quad (4)$$

3 Generation of HO_2^- and its decomposition after the removal of α-oxide:

$${}_{ads}(O_2^-)Au(OH)_3...(\ PhO^-) + H_2O + e^- \rightarrow {}_{ads}(HO_2^-) Au(OH)_3...(\ PhO^-) + HO^- \quad (5)$$

$${}_{ads}(HO_2^-)Au(OH)_3...(\ PhO^-) \rightarrow Au(OH)_3...(\ PhO^-) + HO_2^- \quad (6)$$

$$Au(OH)_2 + e^- \rightarrow Au(OH) + HO^- \quad (7)$$

where $Au(OH)_2$ designates α-oxide

$$Au(OH) + 2\ HO_2^- - 2e^- \rightarrow Au(OH)_3 + 2O^\bullet \quad (8)$$

4 Phenoxy radical formation and oxidation:

$$Au(OH)_3...(\ PhO^-) \rightarrow Au(OH)_3^- ...PhO^\bullet \quad (9)$$

$$Au(OH)_3^- ...PhO^\bullet + O^\bullet \rightarrow Au(OH)_2 + BQ + H_2O \quad (10)$$

In the potential range from 1.05 to 1.57 V the tentative reaction path including Equations 9 and 11 describes the anodic processes at the overlayer surface:

$$Au(OH)_3^-...PhO^\bullet + 2HO^- - e^- \rightarrow Au(OH)_2 + BQ + 2H_2O \quad (11)$$

The above reaction schemes reveal that the redox couple Au(I)/Au(III) is involved in the oxidation of phenol in the potential range from 1.05 V to 2.50 V. In the absence of evolved O_2, the process is not cyclic and the Au(III)-ion participates in the oxidation, the rate for which is decaying due to the consumption of β-oxide. The formation, oxidation and dimerization of phenoxy radicals may be visualized by the structural reactions presented in Figure 11. A long-term electrolysis has been performed with a preanodized gold electrode at 2.5 V in the absence of additives. A large peak in the vicinity of about 270–280 nm characterizes the absorption spectrum of analysed samples recorded by a UV-VIS spectrophotometer (Perkin Elmer Lambda 2). This behaviour is characteristic of p-benzoquinone. The more reactive o-benzoquinone is subjected to deeper oxidative transformation. Similar conclusions were deduced by A. von Mengershausen *et al*, for the electrochemical oxidation of phenol promoted by incipient hydrous gold oxides in an acidic medium (24).

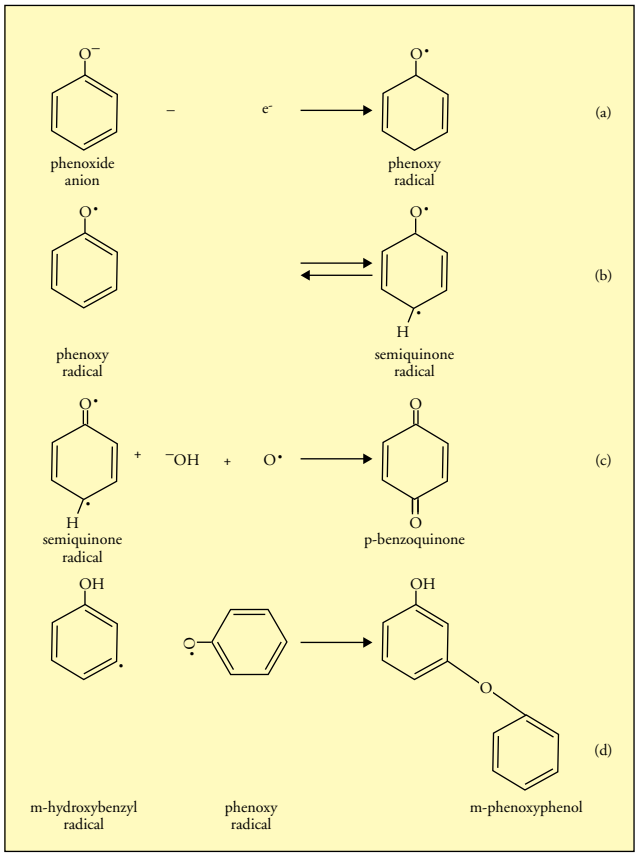

Figure 11 *Simplified scheme of phenol (PhOH) oxidation and dimerization pathways*

In the presence of added KCl or $KClO_4$ the values of i_p are lower (see Figures 6a and 6b). Based on the apparent activation energies found in presence of KCl (70.6 kJ mol^{-1}) and $KClO_4$ (69.4 kJ mol^{-1}), indirect transformation of phenol involving another electrochemically generated reagent may be suggested. The two values are very close and this shows that the processes occurring are of a very similar nature. From the diagram E-pH (12) for the metastable chloride-water system, KCl and $KClO_4$ are present as ClO^- at E_l higher than 1.0 V and at pH > 12. Thus, ClO^- is assumed to undergo electrochemical decomposition with $Cl^\bullet$ generation, which further interacts with $PhO^\bullet$ to give monochlorophenol as a side product. This is supported by the well-known fact that ClO^- acts as an oxidizing and chlorinating agent for organic compounds (25). Anodic oxidation of phenol in the presence of NaCl has been studied previously (26) and the formation of chlorinated organics had been reported. According to Comninellis and Nerini, in presence of NaCl the phenol oxidation process occurs *via* ClO^- generated near to the anode or/and in the bulk of the solution, and the chlorinated phenols obtained are oxidized further to aliphatic acids (27).

Our experiments are focused on the study of the mechanism of phenol oxidation on potentiostatically grown gold oxide films with and without additives and not at the industrial aspects of the process. To increase the thickness of β-oxide grown at the polarization stage, very high concentrations of $KClO_4$ and KCl were used in this study. At lower concentrations of the additives, parallel chlorination and oxidation reactions occur with corresponding activation energies of *ca* 70 kJ mol^{-1} and 17 kJ mol^{-1}. The four-fold difference in these values indicates that the latter process predominates.

Noble metal catalysts are not yet used for the removal of organic pollutants in wastewater. The stability and high catalyst price may be given as a major reason. Future industrial applications may involve carbon supported noble metal oxide catalysts, promoted by oxides of different heavy metals, as mixed oxide catalysis is more efficient (28). Carbon supported platinum was used in previous studies (29); but platinum is a poor electrode material for the further oxidation of BQ intermediate as it adheres strongly to the electrode surface during the adsorption stage. This is why other metal catalysts such as gold, which allow desorption of the intermediates and faster turnover of electrode surface are more promising for future studies.

CONCLUSIONS

Potentiostatically grown pc-gold oxide films have been studied using cyclic voltammetry in basic aqueous solutions. It has been shown that phenol is oxidized only in the range of 1.05 - 2.50 V, which provides β-oxide on the electrode surface, and the products of oxygen reduction act as phenol oxidants. The depletion of β-oxide is accompanied by rapid electrode passivation. A tentative reaction mechanism has been proposed on the basis of the incipient hydrous oxide/adatom mediator (IHOAM) model of electrocatalysis. It accounts for the participation in the oxidation of phenol of Au(I)/Au(III) as a redox mediator couple.

The effects of added $KClO_4$ or KCl on the thickness of the potentiostatically grown oxide film and its catalytic effect on the nature of the chemical reactions taking place has been studied. In solutions having a high concentration of added $KClO_4$ or KCl and short reaction times chlorination occurs at gold oxide films. At lower concentrations of the additives and longer

reaction times, only oxidation occurs since the activation energy of the process is considerably lower.

ACKNOWLEDGEMENT

The financial support by the Bulgarian National Science Fund through grants TH 527 and X-712 is gratefully acknowledged.

ABOUT THE AUTHORS

Professor Philip Iotov is an affiliate of the University of Chemical Technology and Metallurgy in Sofia. He has worked in the Chemical Engineering, Environmental Engineering, and Fundamentals of Chemical Technology Departments. He obtained his PhD from the Higher Institute of Chemical Technology in Sofia in 1975. Dr Iotov has worked in Tongji University, Shanghai, and The Queen's University, Belfast on environmental science and engineering topics. His publications are related to the study of catalytic processes, including the effect of potentiostatically grown gold oxide films on the oxidation of phenol in basic solutions: research which is relevant to electrocatalysis and wastewater treatment.

Sasha Kalcheva is also a graduate of the Higher Institute of Chemical Technology in Sofia. She received her PhD in 1975. Later she worked on electrocatalysis with Professors Wolf Vielstich and Joachim Heitbaum in Bonn University. Professor Kalcheva has been involved in extensive investigation of the electrocatalytic oxidation of organic substances.

REFERENCES

1 A. Savall, *Chimia*, 1995, **49**, 23
2 M. Gattrell and D.W. Kirk, *J. Electrochem. Soc.*, 1993, **140**, 1534
3 K. Scott, *Proc. Electrochem. Soc.*, 1994, **19**, 51
4 S. Trasatti, *Int. J. Hydrogen Energy*, 1995, **20**, 835
5 L.D. Burke and P.F. Nugent, *Gold Bull.*, 1998, **31**, 39
6 L.D. Burke and P.F. Nugent, *Gold Bull.*, 1997, **30**, 43
7 G. Jerkiewicz, in 'Interfacial Electrochemistry', ed. A. Wieckowski, M. Dekker, New York, 1998
8 G. Tremiliosi-Filho, L.H. Dall' Antonia and G. Jerkiewicz, *J. Electroanal. Chem.*, 1997, **422**, 149
9 P.I. Iotov and S.I. Kalcheva, *Bull. Electrochem.*, 2000, **16**, 407
10 M. Noel and K.I. Vasu, 'Cyclic Voltammetry and the Frontiers of Electrochemistry', Aspect Publ. Ltd., London, 1990, p. 223
11 'CRC Handbook of Chemistry and Physics', 65th Edition, ed. R.C. Weast, CRC Press, Boca Raton, USA 1984, D-155
12 G.H. Kelsall, N.J. Welham and M.A. Diaz, *J. Electroanal. Chem.*, 1993, **361**, 13
13 D. Dickertmann, J.W. Schultze and K.J. Vetter, *J. Electroanal. Chem.* 1974, **55**, 429
14 B.E. Conway, *Prog. Surf. Sci.*, 1995, **49**, 331
15 S.I. Bailey, I.M. Ritchie and F.R. Hewgill, *J. Chem. Soc.* Perkin Trans. II, 1983, 645
16 M. Fleischmann, I.R. Hill, H. Mengoli and M.M. Musiani, *Electrochim. Acta*, 1983, **28**, 1545
17 T.A. Kharlamova and G.A. Teodoradze, *Usp. Khim.*, 1987, **36**, 29
18 C. Paliteiro, *Electrochim. Acta*, 1994, **39**, 1633
19 F.A. Cotton and G. Wilkinson, 'Advanced Inorganic Chemistry', 3rd Edition,, J. Wiley & Sons Inc., New York *etc*, 1972
20 L.D. Burke and V.J. Cunnane, *J. Electroanal. Chem.*, 1986, **210**, 69
21 L.D. Burke, J.K. Casey, J.A. Morrissey and M.M. Murphy, *Bull. Electrochem.*, 1991, **7**, 506
22 L.D. Burke, D.T. Buckley and J.A. Morrissey, *Analyst*, 1994, **119**, 841
23 L.D. Burke, G.M. Burton and J.A. Collins, *Electrochim Acta*, 1998, **44**, 1467
24 A.A. von Mengershausen, S.M. Esquenoni, C.R. Abaca, S.M. Zaniolo, R.A Nocetti and M.G. Susterisic, '3rd International Symposium on Electrocatalysis', ed. S. Hocevar, M. Gaberscek and A. Pintar, Portoroz, Slovenia, September 11–15 1999, p. 153
25 E. Plattner and C. Comninellis, in 'Process Technologies for Water Treatment', ed. S. Stucki, Plenum Press, New York, 1988, p.205
26 J. Mieluch, A. Sadkowski, J. Wild and P. Zoltowski, *Przem. Chem.*, 1975, **59**, 513
27 Ch. Comninellis and A. Nerini, *J. Appl. Electrochem.*, 1995, **25**, 23
28 E. Lodowicks and F. Beck, *Chem. Eng. Technol.*, 1994, **17**, 338
29 P.J.M. van Andel-Scheffer, 'Noble Metal Catalysis for the Selective Treatment of Wastewater', OSPT Projects, Eindhoven, Netherlands, 1995